



# Newsletter

July 2002

## Introduction/Status

### **XMaS funded until 2007!**

EPSRC announced a new 5 year grant (September 2002-7) for the beamline project at the end of May. We are particularly pleased that our request for a third beamline scientist was supported, as was the purchase of both a position sensitive detector and the proposed 4T magnet. We titled the grant application "New Science on XMaS" and it is indeed the diverse and developing research programmes proposed by the community of XMaS users which elicited strongly supportive comments from the EPSRC referees and the backing of the panel. In 1996 we produced an application that was strongly focussed on traditional diffraction studies of magnetic materials. This time in addition we have a growing community working on bilayers, self-assembled structures, thin films, multilayers, even biological tissue, as well as many types of single crystal materials. We thank all of you, together with the members of our Project Management Committee who provided the scientific case and helped us refine the successive drafts of the application until it achieved near perfection. We were delighted to see such wonderful EPSRC referee's reports!

It was not just the EPSRC who had good opinions of us; the ESRF review of XMaS was also very supportive. One of their suggestions was for closer cooperation between ourselves, the Staff of ID20 and theoreticians including the ESRF Theory Group. With this in mind we are organising a one-day Magnetism Workshop on Friday 13<sup>th</sup> September. Paul Strange (Keele University) is our Scientific organiser and details about the programme will soon be on our web

site or available from [s.beufoy@warwick.ac.uk](mailto:s.beufoy@warwick.ac.uk). In previous issues of the Newsletter we have described new facility upgrades that had either been introduced or were imminent. We are now pleased to say that we do indeed have a motorised x-y-z stage working to our original specification. In fact it is so good that it has been pronounced indispensable for manipulating all samples, not just those held in a cryostat, and therefore we are ordering another one to insure XMaS operation against goniometer crashes. The phase plate has been used to good effect by groups studying magnetic multilayers and we are close to having our 1.7K cryostat operating at any inclination to the vertical, including upside down!

*Malcolm Cooper & Chris Lucas*



*The new xyz cryostat mount, in routine use since March*



THE UNIVERSITY  
of LIVERPOOL

 *is an EPSRC sponsored project*



THE UNIVERSITY OF  
WARWICK



The photograph above was taken during the discussion session of the XMaS Workshop, held at Liverpool University in December

## Some Recent Experiments

### Disordered charge stripes in $\text{La}_{2-x}\text{Sr}_x\text{NiO}_4$ ( $0.2 < x < 0.33$ )

*M. E. Ghazi, S. B. Wilkins, P. D. Spencer, P. D. Hatton, P. Prabhakaran, A.T. Boothroyd - for further information contact P. D. Hatton at Department of Physics, University of Durham, DH1 3LE, U.K. (p.d.hatton@dur.ac.uk)*

Lanthanum nickelate ( $\text{La}_2\text{NiO}_4$ ) is a rather dull antiferromagnetic insulator. However the random substitution of lanthanum by strontium causes dramatic changes to the physical properties and a number of structural and electronic effects that are only now being understood. The substitution of a trivalent cation ( $\text{La}^{3+}$ ) by a divalent one ( $\text{Sr}^{2+}$ ) is akin to adding a hole to the lattice. The  $\text{Sr}^{2+}$  is static, but the hole is free to migrate throughout the lattice and, just as in conventional semiconductors like silicon or gallium arsenide, it is the mobile holes that cause the physical properties to be so radically changed. In cuprates, for example  $\text{La}_{2-x}\text{Sr}_x\text{CuO}_4$ , high temperature superconductivity is observed, whereas in manganites colossal magnetoresistance is obtained. In nickelates we obtain charge stripes as shown in Figure 1. At low temperature ( $< 240$  K) the holes form long linear chains on the nickel sites that act as antiferromagnetic boundaries between charge (and spin) stripes. The holes cause a disproportionation of the Ni ions into both  $\text{Ni}^{3+}$  ions (between the holes) and  $\text{Ni}^{2+}$  ions. It is these charge stripes that we detect using x-ray scattering.

As the charge stripes are running diagonally with respect to the unit cell, we find that upon cooling additional satellite reflections are formed symmetrically around Bragg reflections at  $(2\varepsilon, 0, 1-\varepsilon)$  where  $\varepsilon$  is the concentration of holes. Thus measurement of the position and width of these satellites provides information about the stripe separation and order as a function of temperature. In an earlier study at XMaS we had determined that, in the special case of  $x = 1/3$ , the commensurate charge stripes were two-dimensional and that above  $T_C$  there were spatial charge fluctuations. Next we wanted to know what happens for other concentrations of Sr, where the stripes cannot fit commensurably with the lattice. To answer this question a series of high quality crystals were grown at Oxford University in an image furnace. We undertook a series of measurements on crystals with strontium concentrations  $x = 0.2, 0.25, 0.275, 0.30$  and  $0.33$ . The separation of the stripes broadly followed the Sr concentration: as the Sr concentration, and hence number of holes, decreased, the separation of the stripes increased (in direct space). However we found the wavevector,  $\varepsilon$ , to be incommensurate, and to vary with temperature as shown in Figure 2. At low temperatures the incommensurability parameter,  $\varepsilon$ , depends primarily upon the Sr concentration. However it does not lock-in at commensurate values like  $0.25$ , where there would be domain walls every four unit cells. As the



temperature is raised thermal energy causes the stripes to vibrate with greater and greater amplitude and the Coulomb repulsion is overcome, dragging the stripes closer together. Indeed at high temperatures, well above the charge ordering temperature, the stripe separation within the spatial charge fluctuations is observed to increase rapidly to the value of  $\epsilon = 1/3$ .

The Sr concentration and temperature also affect the long-range correlation of the stripes. Measurement of the width of the charge stripe satellites at high resolution (using an Si analyser) gives an indication of the inverse correlation length and hence the long range correlation of the stripes. At  $x = 1/3$  the stripes satellites are very sharp and hence ordered over many unit cells. This correlation drops dramatically as the charge stripes melt at  $T_C$ . However, as the hole concentration is decreased the correlation length of the stripes also decreases as shown in Figure 3. Indeed for  $x = 0.2$  the stripes are only ordered over a few unit cells – a charge stripe glass. Further studies are planned to investigate the effect of adding more holes, with Sr concentrations in the range 0.4 – 0.7. It is believed that the half doped material with  $x = 1/2$  may be a special commensurate composition like  $x = 1/3$ .

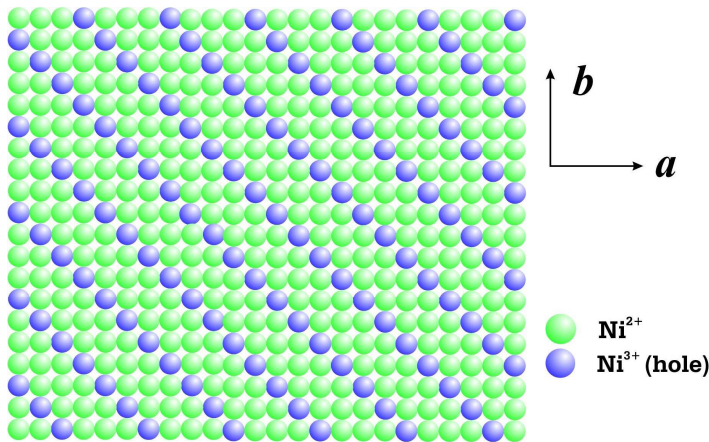


Figure 1 : Direct space ordering of holes at low temperature in  $\text{La}_{5/3}\text{Sr}_{1/3}\text{NiO}_4$

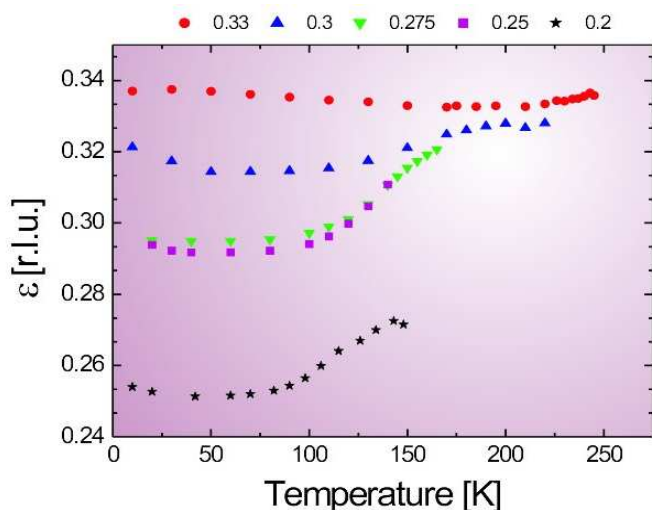


Figure 2 : Variation of the correlation length as a function of temperature for a variety of crystals of  $\text{La}_{2-x}\text{Sr}_x\text{NiO}_4$ .

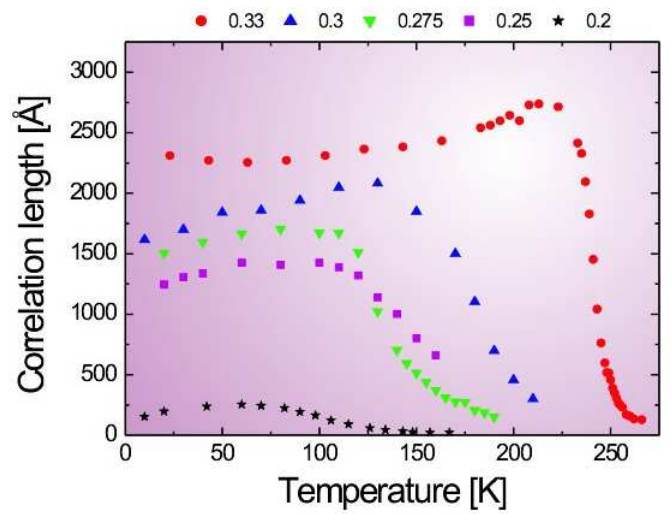


Figure 3 : Variation with temperature of the charge stripe spacing in the  $a^* - b^*$  plane.

## Resonant Ferromagnetic Diffraction from Uranium Sulphide

*D. Laundy, S. Collins, L. Bouchenoire, S. Brown, P. Thompson— for more information contact D. Laundy at Daresbury Laboratory, Warrington WA4 4AD, UK [d.laundy@dl.ac.uk](mailto:d.laundy@dl.ac.uk)*

At x-ray energies near the uranium M-edges, a magnetic Bragg peak can be enhanced by a factor of order  $10^6$  and thus resonant diffraction has frequently been used to study antiferromagnets. With ferromagnets, the charge and magnetic Bragg peaks are coincident and so there is the additional possibility of interference between the charge and magnetic amplitudes. An x-ray beam linearly polarised in the horizontal plane, was used for this study of US on XMaS. The electromagnet was mounted with the magnet field in the vertical direction and scattering near to  $90^\circ$  in the horizontal plane was measured. In this geometry, the incident beam has  $\pi$  polarisation and there is interference between the charge and the magnetic amplitude in the  $\pi$  channel of the scattered beam (for charge scattering,  $\pi$ - $\sigma$  scattering is not allowed). The single crystal sample was studied at temperatures above and below the Curie temperature (180K). Figure 2 shows the intensity of the (0,0,2) reflection at 130K for field up and field down. When the energy is equal to the  $M_{IV}$  resonance energy, there is strong cancellation between the charge and magnetic amplitudes resulting in almost zero intensity for the field down. It should also be noted that the Bragg angle was close to  $45^\circ$  and so the Bragg amplitude was already reduced due to the beam polarisation. The ferromagnetism also causes strain within the crystal lattice. This strain causes splitting in the (1,1,1) peak which disappears when the temperature is at  $T_C$ .

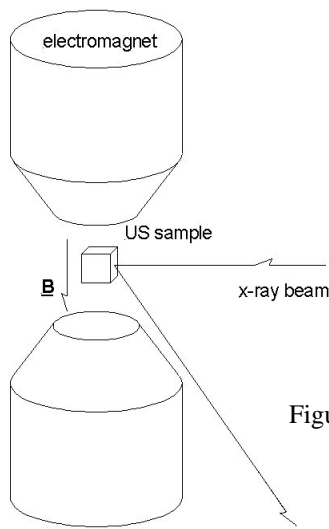


Figure 1

### Scattering from Ferromagnetic US.

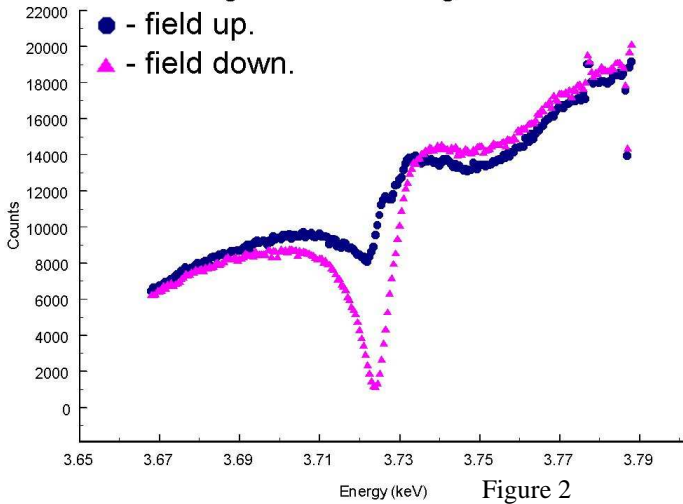


Figure 2

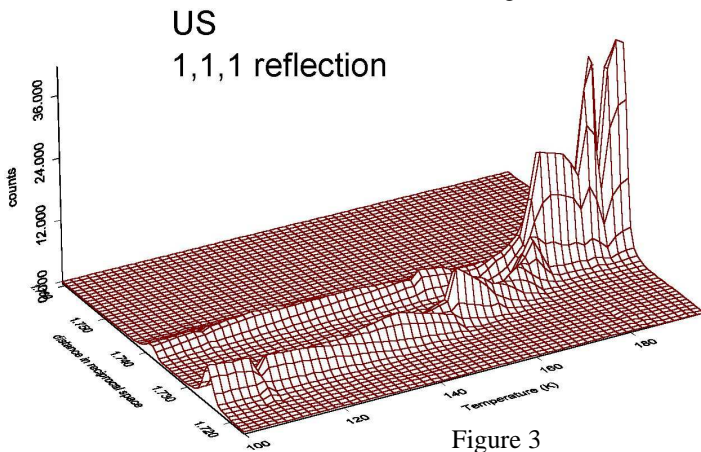


Figure 3

## The Structure of Si/Ge<sub>x</sub>Si<sub>1-x</sub> Superlattices and Quantum Dots

R. A. Cowley, A. Babkevich, M. Bentall, S. Brown and D. Mannix—for further information contact A. Babkevich at Clarendon Laboratory, University of Oxford, Oxford OX1 3PU, UK. [a.babkevich1@physics.oxford.ac.uk](mailto:a.babkevich1@physics.oxford.ac.uk)

One of the most topical areas in semiconductor physics concerns the properties of quantum dots and their possible technological applications. The full exploitation of quantum dots requires that they be regularly spaced on a surface or preferably in a three

dimensional lattice. One of the ways of achieving this, in systems with large lattice mismatch (eg Si/Ge), is to grow *wavy superlattices*. These have the thickness and concentration of the Si/Ge alloy varying laterally along the superlattice and are coherent from one layer to the next. X-ray diffraction experiments permit the determination of the wavelength of the modulations and also the size and strain of the quantum dots.

At XMaS we have studied Si/Ge<sub>x</sub>Si<sub>1-x</sub> superlattices, exhibiting wavy interfaces, grown by MBE on Si substrates at the Institute of Microstructural Sciences in Ottawa. The samples had a wide range of Ge composition -  $x = 0.37, 0.46, 0.56$  corresponding to periodicities of 157 Å, 174 Å, 166 Å respectively. Two different wavelengths, 1.13 Å and 0.62 Å were used to measure the x-ray scattering for wave-vector transfers near a few symmetrical and asymmetrical reflections. Scans were performed by varying the wave-vector transfer along the [110] and [001] directions and by reciprocal space mapping. The maps near the on-axis (004) reflection (Figure 1) and off-axis (115) reflection are shown in figures 1 and 2 respectively.

They indicate a high quality superlattice that is perfectly lattice-matched to the substrate. Figure 3 is a typical scan through one of the superlattice peaks near the (004) Bragg reflection when the wave vector transfer,  $\mathbf{K}$ , changes along the [110] direction. The two strong side peaks originate from the periodic arrangement of 'dots' in the wavy superlattice. The spacing between the peaks indicates an average dot periodicity of about 1500 Å and the width of the peaks corresponds to a coherence length of 1400 Å. Similar measurements near the other Bragg reflections confirm the scattering is from the 'dots' rather than that from dislocations or other imperfections. Further analysis is in progress that should provide detailed information about the in-plane structure of the dots.

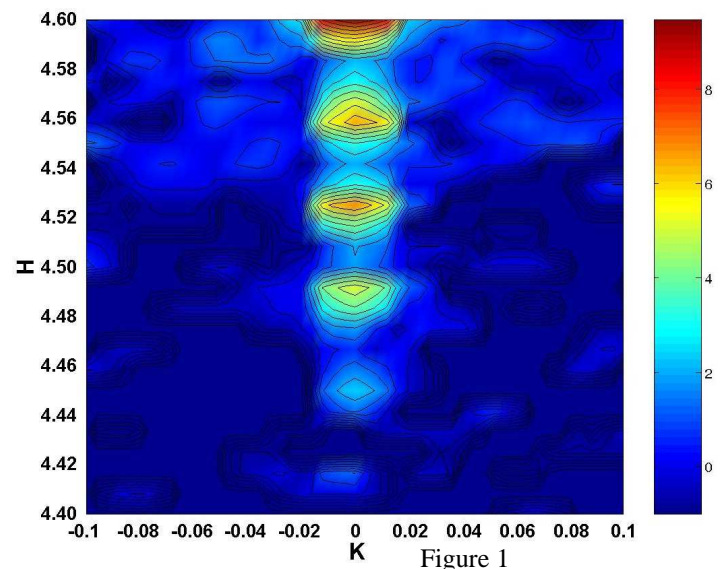


Figure 1



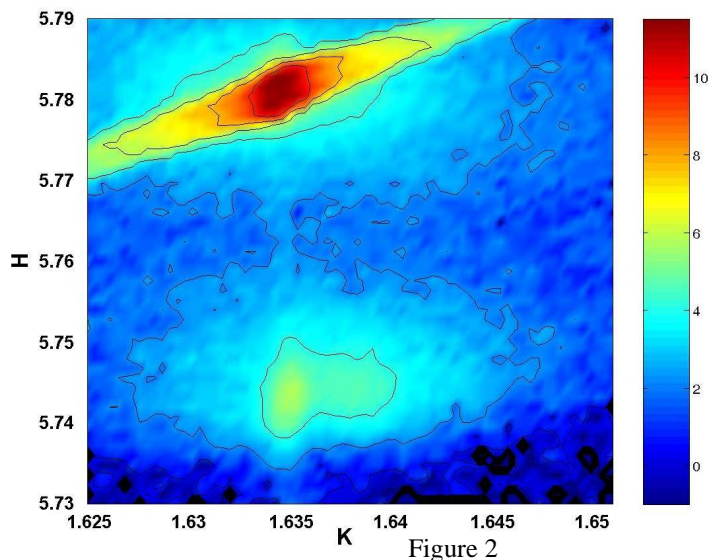


Figure 2

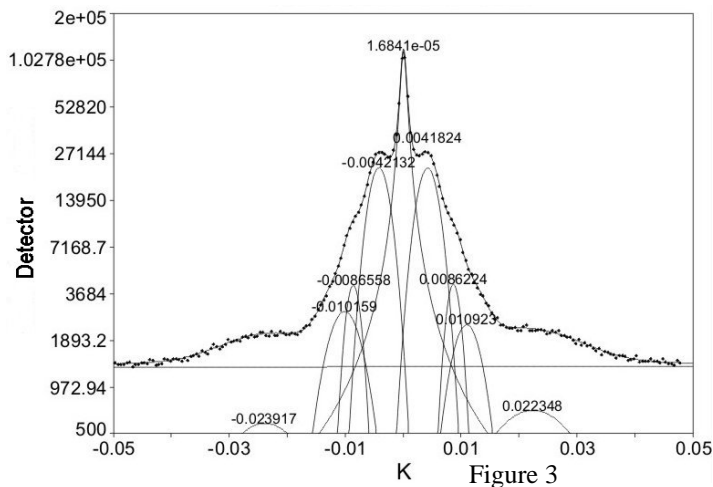


Figure 3

magnetic anisotropy. The large  $5f$  orbital moment leads to large Magneto Optic Kerr Effects (MOKE), which coupled with the possibility of perpendicular magnetic anisotropy, has potential application in high-density optical data recording.

We can now produce U/Fe multilayers by DC sputtering and their high quality has recently been confirmed by x-ray reflectivity measurements (see Figure 1). The fitting model for the resultant spectra (for a nominal  $[U30\text{\AA}/Fe40\text{\AA}]_{\times 30}$  multilayer) included low-density bi-layers at the substrate and air interfaces. The remaining 28 bilayers were modelled with uniform densities close to tabulated values, and constant thicknesses, indicating a well-ordered stack. The structure in the diffuse scatter is indicative of conformal roughness.

Spin dependent reflectivity spectra have also been obtained at the U  $M_{IV}$  edge (3.728 keV). Using a 0.3 mm thick diamond (111) phase plate in Laue transmission 99.7 % circular polarisation was achieved. A 1 T field was applied along the incident beam direction and periodically reversed. The asymmetry ratio, measured at the first superlattice peak at 10 K, is shown in Figure 2. There is a clear peak at 3.728 keV, despite the poor statistics, indicating the existence of a U moment. Work is continuing on this and other samples.

## Resonant magnetic reflectivity from U/Fe multilayers

*S. Brown, S. Langridge, W. Stirling, G. Lander, A Herring, M. Thomas, S Zochowski, P. Thompson, L. Bouchenoire, A. Mirone - for further information contact S. Brown at XMaS, BM28, ESRF, Grenoble sbrown@esrf.fr*

Many elements have been used in the fabrication of magnetic multilayers. The incorporation of 3d elements into the multilayer stack often provokes Giant Magneto Resistance (GMR), notably in Fe/Cr. The development of rare-earth multilayers has stimulated much interest with perhaps the most unusual properties arising when cerium is a constituent. Because its  $4f$  electrons tend to be delocalised there is a strong reaction with any  $3d$  electrons, for example, in Ce/Fe multilayers. A natural extension of the present multilayer research is the placement of  $5f$  electrons in these structures. Their wide range of magnetic properties, from localised magnetism (e.g. in  $UO_2$ ) to itinerant ferromagnetism (e.g. in  $UFe_2$ ) make this a rich and potentially important field. Many uranium compounds are magnetic and exhibit strong hybridisation and large

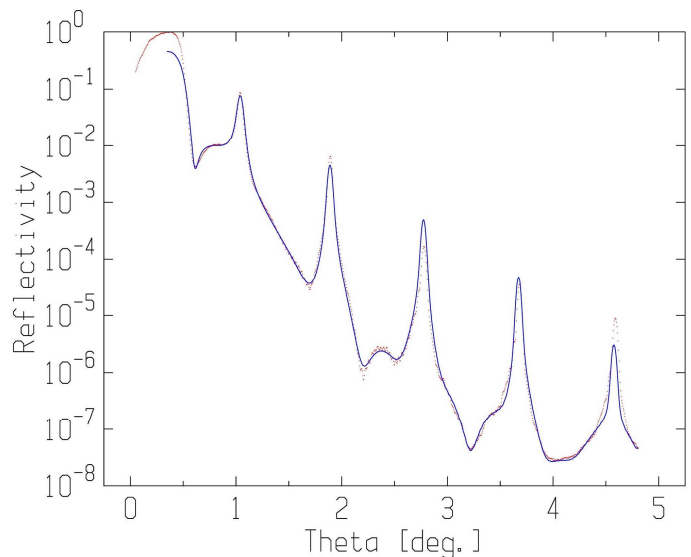
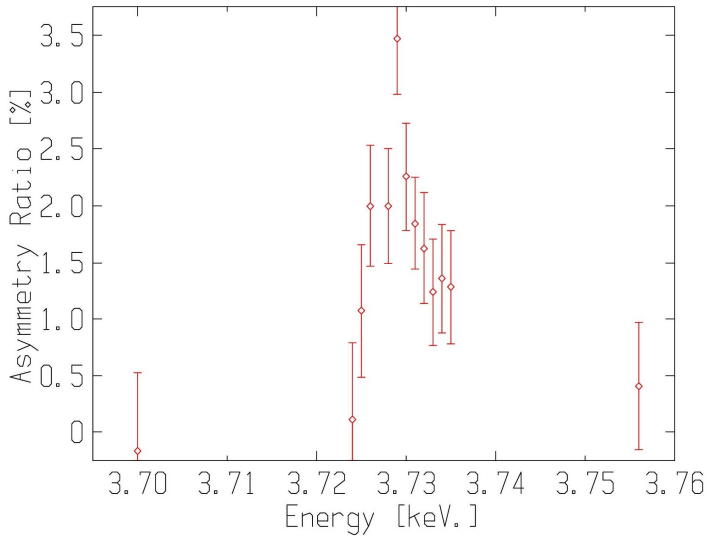


Fig 1. Specular reflectivity (dots) and a fit described in the text (line).



**Fig 2.** Asymmetry ratio indicating a ferromagnetic moment on the Uranium

## Coexistence of charge density waves and antiferromagnetism in $\text{Er}_5\text{Ir}_4\text{Si}_{10}$

*F. Galli, R. Feyerherm, R. W. A. Hendriks, E. Dudzik, S. D. Brown, G. J. Nieuwenhuys, S. Ramakrishnan, S. Van Smaalen, J. A. Mydosh - for further information contact F. Galli, Kamerlingh Onnes Laboratories, Leiden, The Netherlands*

*galli@phys.leidenuniv.nl*

Investigations of electronic phase transitions, such as charge density waves (CDWs), require synchrotron radiation. Moreover, resonant scattering techniques can be employed to investigate magnetic transitions. We have studied CDWs and local moment antiferromagnetism (LM-AFM) on a high-quality single-crystal of the intermetallic compound  $\text{Er}_5\text{Ir}_4\text{Si}_{10}$  at XMaS, and have successfully established the coexistence of the two phenomena. Previous studies have shown that a first transition at  $T_{\text{CDW}} = 151$  K involved the development of a combined commensurate [ $q = (0,0,1/2)$ ] and incommensurate [ $q = (0,0,1/4 \pm \delta)$ , where  $\delta$  is the incommensurability] superlattice. This experiment shows that the commensurate superlattice exhibits large critical scattering above  $T_{\text{CDW}}$ , whereas the incommensurate one does not. Figure 1 shows the FWHM of the commensurate reflection  $(4,4,1/2)$ , the main crystallographic line  $(4,4,1)$  and two incommensurate reflections. The results substantiate a previous idea that the commensurate distortion enhances the nesting that causes incommensurate charge density waves to form. The alternative scenario, that the first is a superposition of the latter, can be excluded.

At the lower temperature ( $T_{\text{LI}} = 60$  K), the incommensurate superlattice becomes commensurate and finally, at the Néel temperature (2.8 K), it becomes antiferromagnetic. The magnetic structure of the localized  $\text{Er}^{3+}$  moments had previously been

determined by neutron diffraction. In the XMaS experiment below 2.8 K we tuned the x-ray energy to the erbium L edge (8.36 keV) and, two significant magnetic Bragg reflections were measured. The temperature dependence of the integrated intensities of these reflections and the comparison with the neutron data is shown in Figure 2. No contribution from the Ir (L edge at 11.21 keV) to the magnetism could be detected. The temperature dependence of the superlattice reflections (CDWs) just above and below the magnetic ordering is also shown in Figure 3. No change in the intensities, or in their position and width, could be detected. This proves that charge density waves and local moment antiferromagnetism coexist in  $\text{Er}_5\text{Ir}_4\text{Si}_{10}$ . The magnetic ordering temperature, on the other hand, may be affected (lowered) by the decreased density of states at the Fermi level, due to the partial gap opened by the CDW.

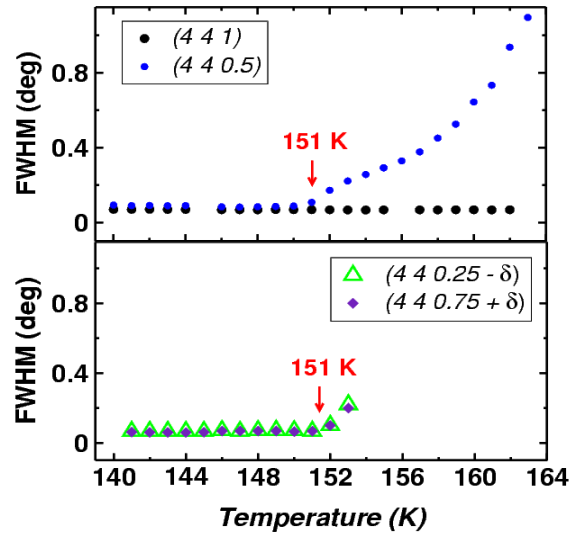


**Figure 1** The line width (FWHM) from omega-scans versus temperature, for  $140 < T < 163$  K. The transition temperature is indicated. The incommensurate reflections (lower plot) disappear above 153~K.

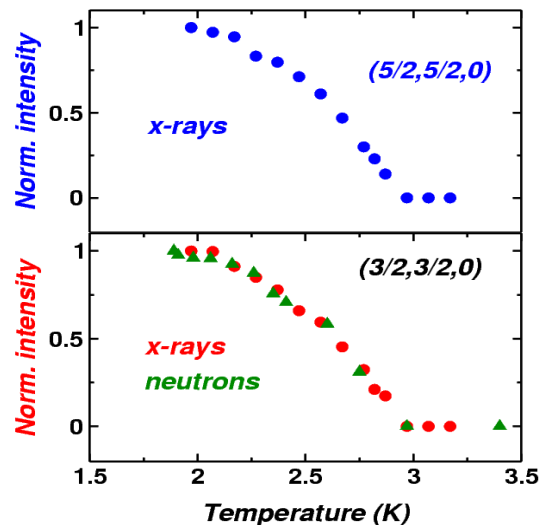


**Figure 2** The temperature dependence of the integrated intensity of resonant magnetic Bragg reflection for: upper plot  $(5/2, 5/2, 0)$ ; lower plot:  $(3/2, 3/2, 0)$  compared with neutron data showing the temperature dependence of the square root of the intensity of the same reflection.

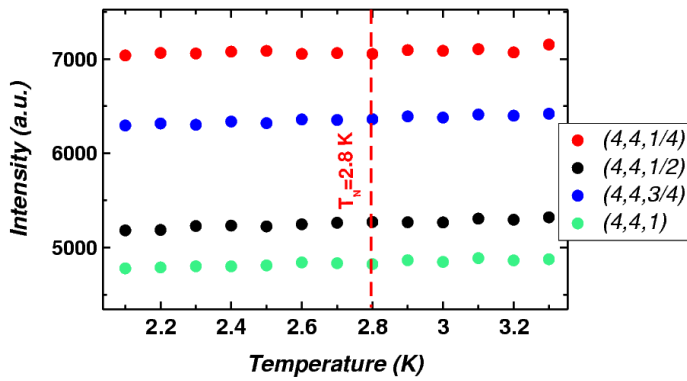


Figure 3 Temperature dependence of the integrated intensities of the superlattice reflections (4,4,1/2), (4,4,1/4), (4,4,3/4) and of the main line (4,4,1) upon cooling below  $T_N = 2.8$  K.

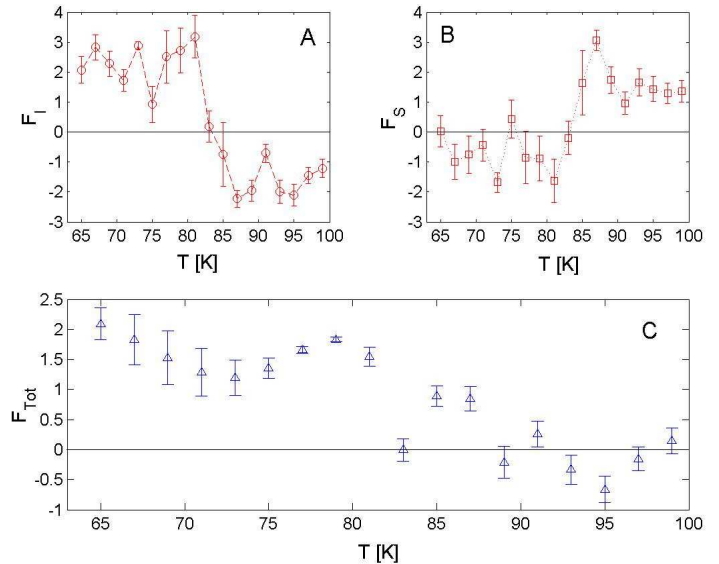
## A ferromagnet with no moment: spin and orbital magnetization compensation in $\text{Sm}_{1-x}\text{Gd}_x\text{Al}_2$

*J.W. Taylor, J.A. Duffy, A.M. Bebb, M.R. Lees, L. Bouchenoire, S.D. Brown, M.J. Cooper, - for further information contact J.A. Duffy, Physics Dept., Warwick University, Coventry CV4 7AL, UK*  
*j.a.duffy@warwick.ac.uk*

The Laves phase compound  $\text{Sm}_{1-x}\text{Gd}_x\text{Al}_2$  has a spin-orbital compensation point at  $\sim 85$  K when  $x = 0.0185$ . The bulk magnetization tends to zero at this temperature, but is finite either side in the magnetically ordered phase (the Curie temperature is 128 K). At the compensation temperature, magnetic Compton scattering shows a net spin moment, indicating that the system consists of a ferromagnetically ordered spin sublattice. For the net moment to be zero, this spin moment must be exactly compensated by the orbital moment. Although it is thought that this may be driven by the different temperature dependencies of the Sm 4f spin and orbital moments, this had not previously been investigated. Therefore we made a direct measurement of the temperature dependence of the spin and orbital form factors of the (3,3,3) reflection of a single crystal sample using non-resonant ferromagnetic diffraction.

The crystalline electric field (CEF), acting on a samarium ion produces a ground state which consist of an admixture of  $J$  states and the population of the 5/2 and 7/2  $J$  states has a greater temperature dependence than observed in other lanthanides. Inclusion of a solid solution of Gd ions introduces a large spin moment and alters the CEF deformation potential, through a small lattice distortion, leading to the spin compensation. By performing non-resonant x-ray diffraction it was possible to separate the components of the moment by varying the magnetizing field direction with respect to the incident and diffracted beams. Elliptically polarised radiation was extracted by viewing the source at a small angle to the electron

orbit plane. The energy of 5.74 keV was selected so that the diffracted beam from the (3,3,3) planes was at  $90^\circ$  in the orbital plane, thereby maximising the magnetic to charge signal ratio. The magnetic form factor was deduced from the change in the Bragg peak intensity when the 1 Tesla magnetic field was flipped (a) parallel to the scattered beam (this gives the total magnetic form factor) and (b) parallel to the incident beam (this isolates the orbital form factor). The advantage of the monochromatic technique over white beam studies pursued on XMaS and elsewhere is a large reduction in the contribution of multiple diffraction. Our results show that the compensation effect is driven by the different temperature dependence of the spin and the orbital moments of the 4f Sm ion. There is a change in sign of both the orbital and spin form factors at the compensation temperature, indicating a distinct change in magnitude of the components of the 4f moment as a function of temperature, which leads to a spin/orbital compensation. The total form factor tends to zero at the compensation point, as expected.



The temperature dependence 333 magnetic form factor of  $\text{Sm}_{1-x}\text{Gd}_x\text{Al}_2$ .

- A: Temperature dependence of the orbital-only form factor.  
 B: Derived spin-only form factor temperature dependence.  
 C: Temperature dependence of the total form factor.

## Structural and Magnetic Interface Morphology of Co/Gd Multilayers

*T.P.A. Hase, J.D.R. Buchanan, B.K. Tanner, J.P. Andres, J.A. Gonzalez, J.M. Riveiro, M.A.L. de la Torre, S. Brown— for more information contact T.P.A. Hase, Department of Physics, University of Durham, U.K.*  
*t.p.a.hase@dur.ac.uk*

Our prime objective was to undertake resonant magnetic scattering using circularly polarized x-rays generated by the new XMaS diamond phase plate. A secondary goal was to elucidate the complex

magnetisation distribution across the Co/Gd interface. Magnetometry studies show that below the Curie temperature of the Gd, the sample behaves as a ferrimagnet with the moments in the layers adopting different configurations as a function of temperature. As the Gd moment orders, it aligns itself in an anti-parallel configuration along the direction defined by the Co moment in an applied field. When the temperature is lowered the Gd moment increases and there exists a compensation temperature when the moments in the adjacent layers are equal. This behaviour could be due to a magnetic dead layer, or related to the interdiffusion processes which are significant in Co/Gd.

Specular and diffuse scattering experiments were undertaken with the x-rays tuned to the Gd  $L_3$  edge ( $E=7.79\text{keV}$ ) for both positive and negative helicity. A difference in intensity was observed on reversal of the helicity of the incident beam at each of the specular Bragg peaks. Grazing incidence scattering experiments were conducted as a function of temperature and field on a sputter deposited Co/Gd multilayer grown on silicon. Figure 1 shows the specular data recorded from a nominal  $[\text{Gd}(50\text{\AA})/\text{Co}(50\text{\AA})]_{*20}$  sample. In agreement with our previous studies we find that a significant portion of the Co layer has interdiffused resulting in the formation of a Gd rich alloy layer [2]. The reduced slightly Curie temperature confirms this hypothesis.

We monitored resonant magnetic scattering by maintaining a fixed scattering geometry, with fixed helicity and conducting experiments as a function of applied field and temperature. Figure 2 shows the flipping ratio at 19.5K. As expected, a signal is only observed at the Bragg peak positions. (NB Upon reversal of the helicity the flipping ratio became equal in magnitude, but opposite in sign for each peak, as expected). The reversal of sign of the flipping ratio between the second and third Bragg peaks shows that the magnetisation distribution within the Gd layer is complex, and is similar to that observed previously in the Fe/Gd system. No variation in the magnitude of the flipping ratio could be observed as a function of applied field at 19.5K. However a weak field dependence was observed for data recorded around the compensation temperature.

As the temperature was increased above 19.5K, a steady reduction in the flipping ratio was observed (see Figure 3), until at compensation, it was no longer measurable. On increasing the temperature to 250K, a signal was again observed, but with opposite sign. These data can be explained assuming the spin configurations shown as insets in Figure 3. However, the exact position of the layer moments around

compensation remain unclear. We have successfully conducted magnetic scattering on the Co/Gd system as a function of temperature and field.

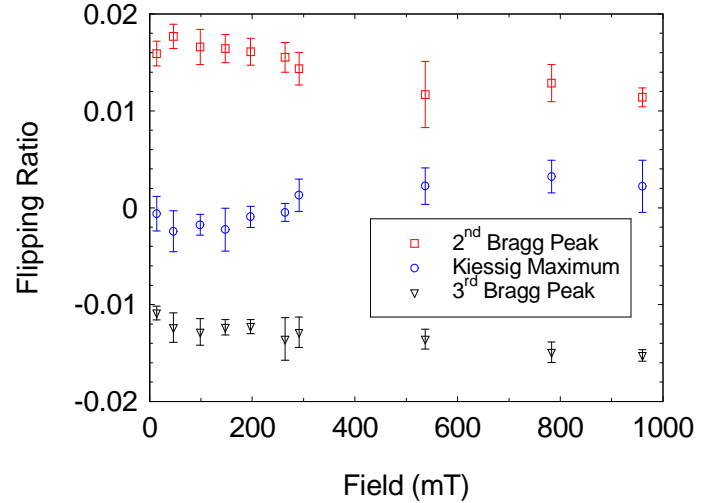


Figure 1: Specular reflectivity (points) and simulation (line) of the Co/Gd multilayer examined.

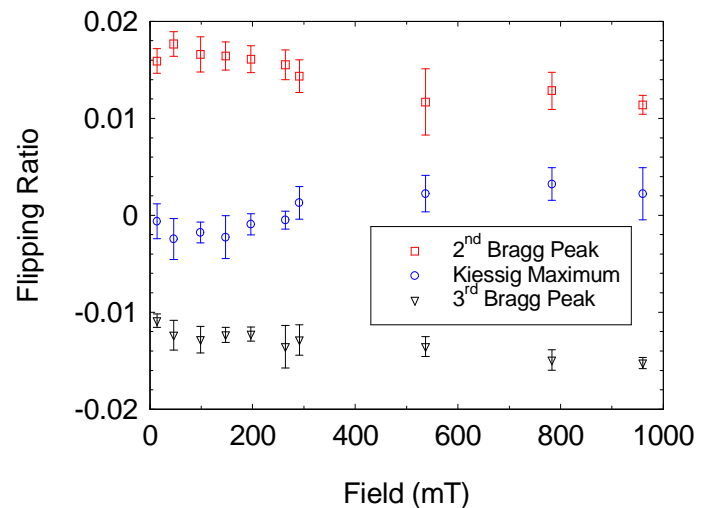


Figure 2: The variation of the flipping ratio with applied field at 19.5K for the 2<sup>nd</sup> and 3<sup>rd</sup> Bragg peaks.

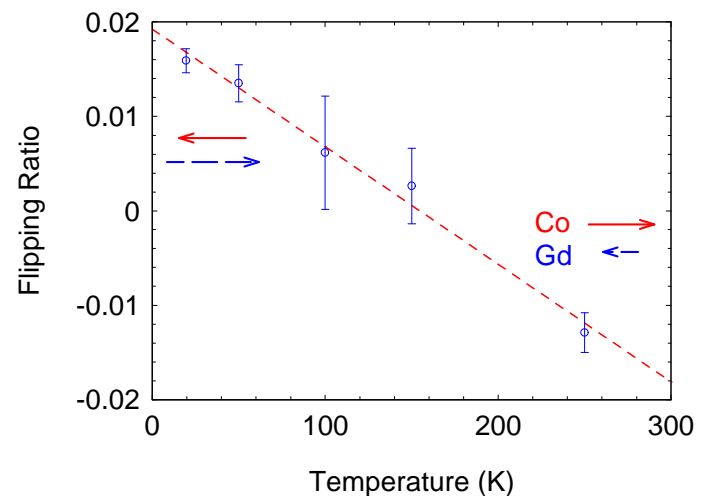


Figure 3: The variation of the flipping ratio as a function of temperature. The layer moment directions are as inset.



## News round-up

The experimental reports in the previous pages are all as yet unpublished. Please email the contact person if you are interested in any of them or wish to quote these results elsewhere.

### Our web site

This is at:

[http://www.esrf.fr/exp\\_facilities/BM28/xmas.html](http://www.esrf.fr/exp_facilities/BM28/xmas.html)

It contains the definitive information about the beamline including experimental report forms and an on-line beamline manual.

### Living allowances

These are now 55 euros per day per beamline user—the equivalent actually paid in pounds sterling, of course. XMaS will continue to support up to 4 users per experiment if you can make a case for the presence of the fourth experimentalist. The ESRF hostel still appears adequate to accommodate all our users, though CRG users will always have a lower priority than the ESRF's own users. Do remember to complete the web-based “A form” requested of you when you receive the ESRF invitation, all attendees must be listed, since this informs the safety group of the attendees and is used to organise all site passes, meal cards and accommodation.

### Beamline people

There have been no changes in the beamline staff since the last Newsletter.

**Project Co-ordinator** - David Paul, (dpaul@esrf.fr), is the person who can provide you with general information about the beamline, application procedures etc. David should normally be your first point of contact.

**Beamline Scientists** - Simon Brown (sbrown@esrf.fr) and Danny Mannix (danny@esrf.fr) continue as beamline scientists **and a third position funded from our new grant will be available in the autumn 2002**, see our web site for details or email our Project Administrator, Sandra Beaufoy (S.Beaufoy@warwick.ac.uk)

**Technical Support** – Congratulations to Paul Thompson (thompso@esrf.fr) on his promotion to Experimental Officer! Paul continues to work on instrument development and provide technical support for the beamline. John Kervin (jkervin@liv.ac.uk), who is based at Liverpool University, provides further technical back-up and spends part of his time on-site at XMaS.

Malcolm Cooper (csmc@spec.warwick.ac.uk) and Chris Lucas (clucas@liv.ac.uk) continue to travel between the UK and France to oversee the operation of the beamline. The administration for XMaS is handled by Sandra Beaufoy at Warwick University (s.beaufoy@spec.warwick.ac.uk).

### HOUSEKEEPING!

We take some trouble to keep the beamline clean and tidy, please leave the beamline in the same state! Samples should be removed from cryostat and other sample environment mounts, tools, etc returned to racks and unwanted materials disposed of in an appropriate manner. When travel arrangements are made, therefore, please allow additional time, at the cessation of beam, to effect a tidy-up.

### LICENCING AGREEMENTS

As a result of developmental work by the beamline staff, licences to manufacture and market three pieces of equipment have been granted to Huber Diffraktionstechnik by the University of Liverpool. These are the tube-slit assembly, the motorised ‘XYZ’ mount and the polarisation analyser. Further details can be found on the beamline website.

### PUBLISH PLEASE!!.....and keep us informed

Although our list of papers reporting work on XMaS is growing we still need more of those publications to appear. We ask you to provide Sandra Beaufoy not only with the reference but also a preprint/reprint for our growing collection. Note that the abstract of a publication can also serve as the experimental report!

### IMPORTANT!

When beamline staff have made a significant contribution to your scientific investigation you may naturally want to include them as authors. Otherwise we ask that you add an acknowledgement, of the form:

“This work was performed on the EPSRC-funded XMaS beam line at the ESRF, directed by M.J. Cooper and C.A. Lucas. We are grateful to the beam line team of S.D. Brown, D.F. Paul, D. Mannix and P. Thompson for their invaluable assistance, and to S. Beaufoy and J. Kervin for additional support.”

## Guidelines for Applying for Beam-time at the XMaS beamline

XMaS Pluo B3, ESRF, BP 220, 38043 Grenoble Cedex, France

Tel: +33 (0)4 76 88 24 36 Fax: +33 (0)4 76 88 24 55

web page : [http://www.esrf.fr/exp\\_facilities/BM28/xmas.html](http://www.esrf.fr/exp_facilities/BM28/xmas.html)

email: [dpaul@esrf.fr](mailto:dpaul@esrf.fr)

### Beamline Operation

The XMaS beamline at the ESRF, which came into operation in April 1998, has some 133 days of beam time available each year for UK user experiments, after deducting time allocated for ESRF users, machine dedicated runs and maintenance days. During the year, two long shut-downs of the ESRF are planned: 5 weeks in winter and 4 weeks in summer. At the ESRF beam is available for user experiments 24 hours a day.

### Applications for Beam Time

Two proposal review rounds are held each year, with deadlines for submission of applications, normally, the end of **March** and **September** for the scheduling periods August to end of February, and March to July, respectively. **Applications for Beam Time** are to be submitted **electronically** (the paper versions are not acceptable) following the successful model used by the ESRF and ourselves. Please consult the instructions given in the ESRF web page:

[www.esrf.fr](http://www.esrf.fr)

Follow the links: “**User Guide**”  
And: “**Applying for Beam Time**”

Follow the instructions carefully — you must choose “XMAS-BM28” and “CRG Proposal” at the appropriate stage in the process. A detailed description of the process is always included in the reminder that is emailed to our users shortly before the deadline —for any problems contact D. Paul, as above.

Technical specifications of the Beamline and instrumentation available are described in the *XMaS* web page.

When preparing your application, please consider the following:

- All sections of the form must be filled in. Particular attention should be given to the safety aspects, and the name and characteristics of the substance completed carefully. Experimental conditions requiring special safety precautions such as the use of lasers, high pressure cells, dangerous substances, toxic substances and

radioactive materials, must be clearly stated in the proposal. Moreover, any ancillary equipment supplied by the user must conform with the appropriate French regulations. Further information may be obtained from the ESRF Experimental Safety Officer, tel: +33 (0)4 76 88 23 69; fax: +33 (0)4 76 88 24 18.

- Please indicate your date preferences, including any dates that you would be unable to attend if invited for an experiment. This will help us to produce a schedule that is satisfactory for all.
- An experimental report on previous measurements must be submitted. New applications will not be considered unless a report on previous work is submitted. These also should be submitted electronically, following the ESRF model. The procedure for the submission follows that for the submission of proposals — again, follow the instructions in the ESRF’s web pages carefully. Reports must be submitted within 6 months of the experiment.
- The XMaS beamline is available for one third of its operational time to the ESRF’s user community. Applications for beamtime within that quota should be made in the ESRF’s proposal round - **Note: their deadlines are earlier than for XMaS! - 1st March and 1st September.** Applications for the same experiment may be made both to XMaS directly and to the ESRF. Obviously proposals successfully awarded beamtime by the ESRF will not then be given beamtime additionally in the XMaS allocation.

### Assessment of Applications

The Peer Review Panel for the UK-CRG considers the proposals, grades them according to scientific excellence, adjusts the requested beam time if required, and recommends proposals to be allocated beam time on the beamline.

Proposals which are allocated beam time must in addition meet ESRF safety and XMaS technical feasibility requirements.

Following each meeting of the Peer Review Panel, proposers will be informed of the decisions taken and some feedback provided.